Phonon interference at self-assembled monolayer interfaces: Molecular dynamics simulations

Lin Hu,[1] Lifa Zhang,[2] Ming Hu,[3] Jian-Sheng Wang,[2] Baowen Li,[2,4] and Pawel Keblinski[1,*]
[1]*Department of Materials Science and Engineering, Rensselaer Polytechnic Institute, Troy, New York 12180, USA*
[2]*Department of Physics and Centre for Computational Science and Engineering, National University of Singapore, Singapore 117542, Republic of Singapore*
[3]*Department of Mechanical and Process Engineering, Institute of Energy Technology, ETH Zurich, 8092 Zurich, Switzerland*
[4]*Graduate School for Integrative Sciences and Engineering, NUS, Singapore 117456, Republic of Singapore*
(Received 16 April 2010; published 18 June 2010)

Using molecular dynamics simulations, we expose phonon interference effects in thermal transports across a self-assembled monolayer (SAM) of alkanethiol molecules covalently bonded to (111) gold substrate and physically bonded to silicon. In particular, we show that the thermal conductance of SAM-Au interface depends on the bonding strength at the SAM-Si interface and that the phonon transmission coefficients show strong and oscillatory dependence on frequency, with oscillatory features diminishing with increasing SAM thickness. To explore the generality of this behavior we analyze a simple model of point junction on a one-dimensional chain using the scattering boundary method.

DOI: 10.1103/PhysRevB.81.235427 PACS number(s): 05.60.−k

I. INTRODUCTION

The invention of electronic devices, such as the diode and transistor, which control and manipulate electrons, has been the main driving force for the fast development of human society in last few decades. The development of devices to control phonons—the carrier of heat in semiconductors and dielectric materials—however, is not as smooth as it is electronic counterpart. The main difficulty lies in the fact that phonons—unlike electrons and photons—are not real particles. Nevertheless, recent years have made headway on new advances. In particular, thermal rectifiers have been designed theoretically[1] with a first experimental realization put forward with help of asymmetric nanotubes[2] and by combining two segments of cobalt dioxide.[3] Moreover, based on the negative differential thermal resistance, a thermal transistor has been proposed[4] which opens the door for the control of phonons. The realization of different thermal logic gates,[5] and thermal memory,[6] has laid the foundation for processing information by phonons. These advances have changed our traditional view about phonons, and a new discipline—phononics—i.e., the science and engineering of phonons has emerged.[7]

In this paper, we shall study another important phenomenon—interference effects. It is well known that interference effects can be used to tailor transmission and reflectance of electromagnetic waves at an interface between two media. In particular, a quarter-wavelength-thick transparent coating can completely eliminate reflection,[8] provided that the refractive index of the coating is given by the geometrical average of the indices of the two adjacent media. However, direct manifestation of the phonon interference is elusive. The primary reasons are that a typical wavelength of phonons that dominate thermal transport is of the order of 1 nm, and that a typical distance over which phonons propagate coherently (phonon mean free path) is of the order of tens of nanometers.[9] These characteristics phonon length scales are nanoscopic, thus our ability to directly observe phonon interference effects similar to that exhibited by optical coatings requires nanoscopic coatings and atomistically smooth interfaces.

To date the most significant efforts in phonon engineering were associated with theoretical analysis and experimental work on superlattices, i.e., alternating multilayers of epitaxially bonded solids.[10–13] Moreover, nanoscale devices like the phonon broadband mirror, color filter, and edge filter were designed to display optimized acoustic reflectivity curves in the terahertz range were grown by molecular beam epitaxy (MBE) technology and characterized by Raman scattering techniques.[13] In the case of superlattices, the phonon interference was shown directly by measuring the transmission coefficient of the phonons.[10] In particular for a 50 layer superlattice sandwich between two solids, it was observed that the transmission coefficient is significantly reduced (to about 30% of the reference value) for certain phonon wavelengths, in manner analogous to that observed in optical systems. The direct demonstration of phonon interference and associated phonon engineering techniques for superlattices include multiple layers of solids (typically tens of more). A demonstration of phonon engineering via use a single molecular layer has not yet been achieved. Furthermore, there is no reported work on phonon interference in the context of the organic layers.

Self-assembled monolayers (SAMs) of organic molecules on gold (111) surfaces[14] are potential candidates for systems where phonon interference can play a direct role. In particular, an interfacial thermal resistance, which is a function of the phonon transmission coefficients,[15] was measured for Au-SAM-GaAs interface.[16] Also, femtosecond laser pulse measurement on SAMs on Au substrate[17] allowed for detailed analysis of heat flow along hydrocarbon chains forming SAM.[18]

In this paper, we will use molecular dynamics (MD) simulations to study heat flow and phonon scattering at Au-SAM-Si interfaces to investigate the role of phonon interference on the transmission of individual phonons and the overall interfacial thermal conductance. We also perform an exact calculation to characterize conduction of point junctions between one-dimensional chains of masses connected

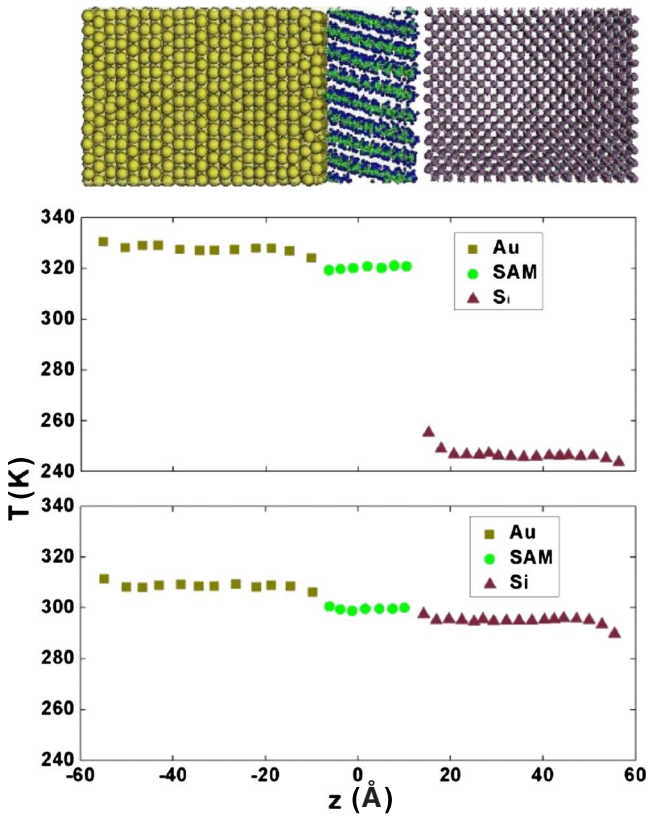

FIG. 1. (Color online) Top panel: snapshot of the Au-SAM-Si structure with 16 C atoms long chains. Middle panel: steady state temperature profile for thermal flux, $J_Q = 800$ MW/m^2 and standard Si-SAM interactions. Bottom panel: same as the middle panel but for five times stronger Si-SAM interactions.

by springs to explore generality of the phonon interference effects in the presence of narrowly spaced multiple junctions and interfaces.

II. MODELS AND MOLECULAR DYNAMICS SIMULATIONS

The model system consists of an SAM composed of alkanethiol [-S-$(CH_2)_{n-1}$-CH_3] chains forming two-dimensional triangular lattice with a surface density of 21.6 Å^2 per chain. The chains form a tilt angle of about 30° with respects to Au surface.[19] The other side of SAM is physically bonded to the hydrogen terminated (100) surface of Si crystal (see Fig. 1).

The structure is contained within a rectangular simulation box with a cross section of 32.6×32.6 Å^2 and a length of about 200 Å, as shown in the top panel of Fig. 1). The silicon crystal is composed of 2304 atoms. The SAM slab contains 48 SAMs chains. We consider several chain lengths involving 3, 8, 16 and 32 carbon atoms. The Au crystal contains 3024 atoms. Periodic boundary conditions are used in the two transverse (x and y) directions. This results in an Si-SAM-Au interface normal to the z direction with outer layers of Si and Au slabs exposed to vacuum.

The interatomic interactions for Si and a hydrocarbon chain are described by the polymer consistent force field (PCFF),[20] which includes both bonded and nonbonded interactions. Only nonbonded interactions (physical bonding) are operative between Si and SAM. The nonbonded interactions are modeled by a short range 9–6 Lennard-Jones (LJ) potential $\varepsilon[[2(\sigma/r)^9 - (\sigma/r)^6]$, where r is the interatomic spacing and the parameters are the energy and length scales, respectively. The LJ potential is truncated and shifted smoothly to zero at a cutoff radius of $r_c = 7.0$ Å. We use the pairwise additive Glue model[21] for the Au-Au interactions and a Morse potential for Au-head group (sulfur) interaction, that reproduce the strength of the thiol bond well.[22] Upon equilibration at 300 K, we observe a tilt angle of about 29°, which agrees very well with the experimental tilt angle of $30 \pm 10°$.[19]

In the first stage of simulations, we equilibrate the system at a constant pressure (1 atm) and temperature of 300 K using Nosé-Hoover thermostat for 1 ns with a MD time step of 0.5 fs. Following the equilibration, we turn off the global thermostat, fix the system volume and apply a velocity rescaling constant rate heat source at the outer side of the Au slab and remove the heat at the same rate at the outer end of the silicon slab, leading to the thermal flux of $J_Q = 800$ MW/m^2. After about 0.5 ns, the steady state was reached and the temperature profiles (see Fig. 1) along the z direction were calculated and averaged over a total of 2.5 ns.

The profiles in the bottom panels of Fig. 1 clearly show that the temperature drops at the Si-SAM and SAM-Au interfaces. The temperature drop, ΔT, relates the thermal interfacial resistance, R, to the thermal flux via,[20]

$$J_Q = \Delta T / R. \tag{1}$$

Thus measuring ΔT we can calculate the interfacial resistance R or equivalently, interfacial conductance $G = 1/R$.

For chain sizes up to 16 carbon atoms, the temperature drop at the Si-SAM and the SAM-Au interfaces are 73 ± 3 and 7 ± 1 K, respectively, corresponding to the interfacial conductance of 11 and 110 MW/(m^2 K). Due to the lack of chemical bonding at the Si-SAM interface, its conductance is much lower that of the SAM-Au interface. The corresponding overall interfacial conductance for the 16 C atom Si-SAM-Au interface is 10 MW/(m^2 K). For the 8 and 32 C long chain, the overall interfacial conductance is 15 and 9 MW/(m^2 K), respectively. This suggests that the conductance decreases with increasing chain length. However, the conductance of the 3 C atom long SAM interface is only 6 MW/(m^2 K), i.e., more than twice lower than for the 8 C atom long SAM interface. This suggests a strong interference effect, perhaps reducing the transmission coefficient of phonons for specific thicknesses of the SAM region.

To provide further evidence for phonon interference effects we increase the L-J potential bonding strength at the Si-SAM interface by a factor of 5 for the 16 C long SAM model. The temperature drop at the Si-SAM interface gets reduced by an order of magnitude to just 5 K, which can be attributed to better interfacial bonding. However, at the SAM-Au interface, the temperature drop increases from 7 to 9 K, despite the fact that the interactions at this interface are not altered. This result clearly indicates that the two inter-

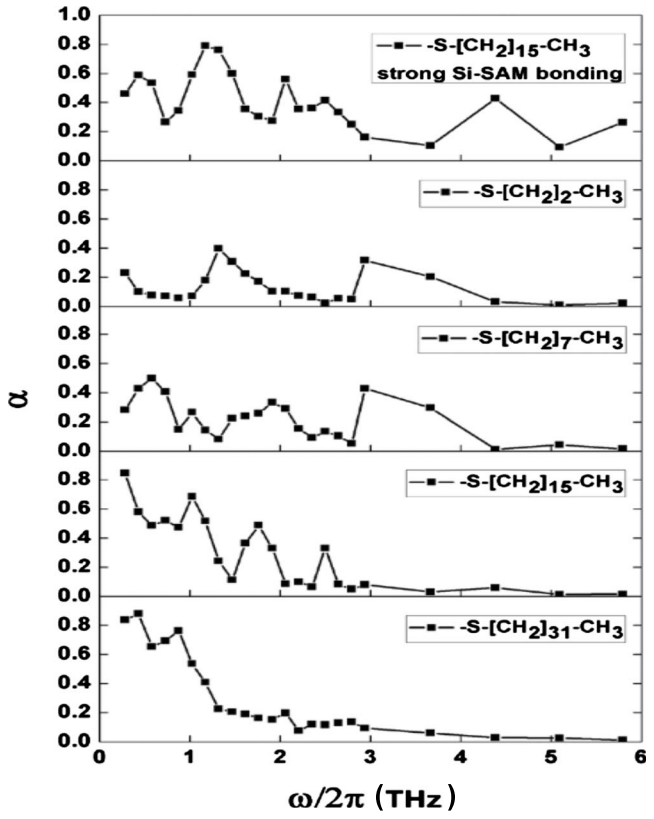

FIG. 2. Energy transmission coefficient α as a function of frequency of the incident LA wave packet for various SAM thicknesses. The top panel corresponds to Si-SAM interactions five times stronger than the standard interaction.

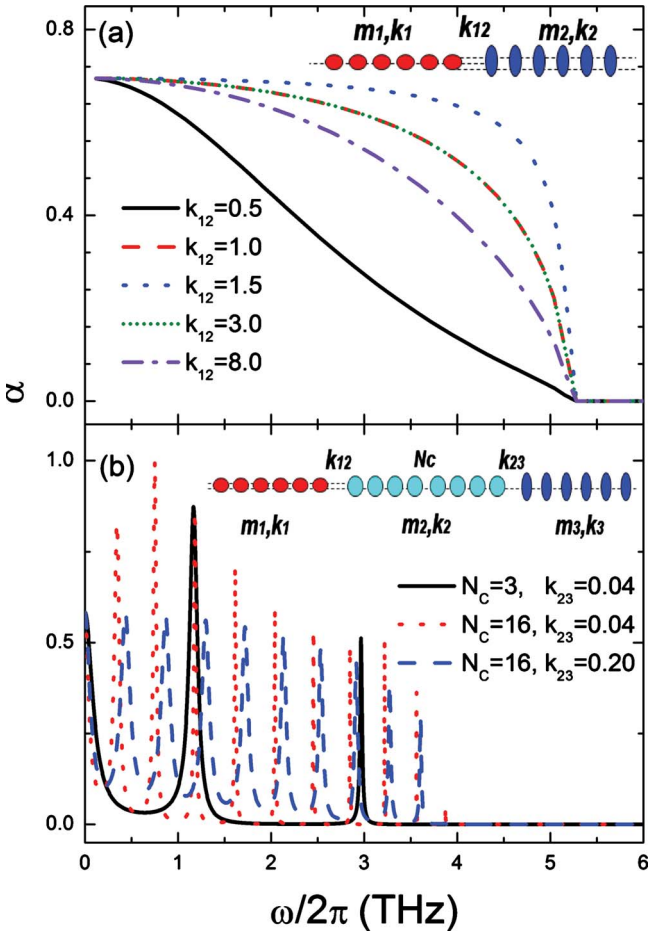

FIG. 3. (Color online) Transmission coefficients as functions of frequency. (a) The transmission in one junction. Two different semi-infinite atomic chains are connected together by parameters as $k_1=1.0$, $m_1=1.0$, $k_2=3.0$, and $m_2=4.0$. The inset is a schematic representation for one-junction case. (b) The transmission in two-junction case which has a center part with N_C atoms connected by two semi-infinite atomic chains. The parameters are $k_1=3.0$, $m_1=7.17$, $k_2=0.3$, $m_2=0.44$, $k_3=1.0$, $m_3=1.0$, $k_{12}=0.20$. The inset is a schematic representation for two-junction atomic chain. Here, for (a) and (b), the unit for coupling k is 16.515 N/m and unit for mass m is 28 amu.

faces are not independent, and due to interference effects, the apparent conductance of one interface depends on the bonding on the other.

We note that the experimentally relevant result is the overall interfacial conductance of the combined Si-SAM-Au interface which is about 15 MW/(m^2 K) for the weak Si-SAM interfaces (except for 3 C atom long SAM) and 60 MW/(m^2 K) for the strong interface. The first value is similar to that measured in Ref. 16, but much smaller than that obtained in Ref. 17. Our results indicate that interfacial interaction strength can greatly affect the interfacial conductance, thus likely explaining discrepancy between various experiments on similar SAM structures.

To provide direct evidence for the phonon interference effects, we perform phonon wave packet dynamic simulations.[23] In the Si crystal we construct spatially localized longitudinal acoustic (LA) wave packets of phonons with well defined frequency, and inject them to otherwise zero temperature relaxed structures.[23] The wave packets propagate toward the interface where they scatter into transmitted and reflected waves. In this simulation we use extended Si and Au slabs with the total simulation cell length of 200 nm. We monitor the dynamical evolution of the wave packet and compute the energy phonon transmission coefficient α, defined as the ratio of energy transmitted across the Si-SAM-Au interface to the energy of the incident wave packet.

The phonon transmission coefficients for various SAM chain sizes are shown in Fig. 2. For all chain sizes, we see an oscillatory behavior with a strong frequency dependence. This is a direct manifestation of phonon interference effects. However, with increasing chain size, the oscillatory features diminish and a monotonic decrease sets in with increasing frequency. Our understanding of this behavior is the following. The interference effects require coherent multiple scattering from the Si-SAM and SAM-Au interfaces. Such coherency is easier to maintain with short SAM molecules. For longer SAM molecules, phonon-phonon scattering diminishes the coherent (ballistic) nature of phonon propagation along the hydrocarbon chain. In consequence, the interference effects are eliminated as the diffusive behavior sets in. We also note that for 3 C long SAM model the phonon transmission coefficients are visibly lower than for other

cases, which is consistent with the fact that this interface has, by far, the lowest conductance.

III. ANALYTICAL MODEL

To underscore the generality of the phonon interference effects involving thin layers sandwiched between two solids, we consider a simple model of a junction structure. By a scattering boundary method within a lattice dynamic approach, which was first proposed by Lumpkin and Saslow to study the Kapitza conductance in one-dimensional lattice[24] and was successfully applied to thermal transport in spin chains,[25] we calculate the phonon transmission coefficients for one-junction and two-junction atomic chains as shown in the inset of Fig. 3. For a one-junction case, we assume a wave solution transmitting from the left lead to the right lead. We label the atoms as $-\infty,\cdots,-1,0,1,2,\cdots,+\infty$. The two media are modeled by atoms with mass m_1 and m_1 connected by springs k_1 and k_2, respectively. An interface is located between atoms 0 and 1 which are connected by a spring k_{12}. From the scattering boundary method, we obtain the continuity condition at the interface as

$$\omega^2 m_1 u_0 = -k_1 u_{-1} + (k_1 + k_{12})u_0 - k_{12}u_1; \tag{2}$$

$$\omega^2 m_2 u_1 = -k_{12} u_0 + (k_{12} + k_2)u_1 - k_{12}u_2. \tag{3}$$

Here u_i is the wave function at the ith atom. For a two-junction case, the transmission wave will be reflected and transmitted by the second boundary, and then the reflection wave will be reflected at the left end again, and then reflected again. At last we obtain the transmission coefficients for one-junction and two-junction cases as

$$\alpha_1(\omega) = 1 - |r_{12}|^2 = 1 - |r_{23}|^2, \tag{4}$$

$$\alpha_2(\omega) = \frac{(1-|r_{12}|^2)(1-|r_{23}|^2)}{|1 - r_{23}r_{21}\lambda_2^{2(Nc-1)}|^2}. \tag{5}$$

Here, N_c is the number of atoms in the center part for two-junction atomic chain; r_{ij} is the reflection coefficient when the phonon wave transmit from part i to part j, which is

$$r_{ij} = \frac{k_i(\lambda_i - 1/\lambda_i)(k_j - k_{ij} - k_j/\lambda_j)}{(k_i - k_{ij} - k_i/\lambda_i)(k_j - k_{ij} - k_j/\lambda_j) - k_{ij}^2} - 1; \tag{6}$$

and $\lambda_i = \frac{-h_i \pm \sqrt{h_i^2 - 4}}{2}$, $h_i = \frac{m_i}{k_i}(\omega + i\eta)^2 - 2$, η is a small positive number: $\eta = 0^+$; m_i and k_i is the mass and spring constant of the ith part of the atomic chain. Here we take one of the two roots: $|\lambda| < 1$, because of the forward moving waves with group velocity $v > 0$.[26]

Using the above explicit formulas, we plot the transmission coefficients as a function of frequency in Fig. 3. Figure 3(a) shows results for a single junction between two semi-infinite atomic chains of different masses and spring constants. The transmission coefficient decreases with increasing frequency for all the coupling k_{12}, which is consistent with the results of MD studies on Si-polyethylene interface.[27] Figure 3(b) shows the transmission as a function of frequency for two-junction models. We find that the transmission coefficient oscillates with the frequency, with the period of oscillations decreasing with increasing junction separation. This is qualitatively the same behavior as observed in our MD simulations of SAM interfaces. In fact, the numbers of peaks are consistent with those in Fig. 2. When we increase the coupling between the center part and right lead k_{23} five times, the transmission coefficient will be lifted in the whole range, which is consistent with the first curve in Fig. 2. All of our results from the scattering boundary method are verified by the nonequilibrium Green's function approach.[28]

IV. SUMMARY AND DISCUSSION

In summary, using MD simulations and scattering boundary method calculations we demonstrate strong phonon interference effects at the nanoscale layers joining two materials. We show that the thermal conductance of one interface depends on the bonding strength at another interface and that the transmission coefficients show a strong and oscillatory dependence on frequency. We use the scattering boundary method to study the generality of the phonon interference effects involving thin layers sandwiched between two solids. Explicit formulas for the transmission coefficient are given for one- and two-junction structures, which are consistent with our MD simulations. Our results demonstrate the potential for phonon filtering, tailored by the layer thickness and interfacial interactions that can be used in design of new interfacial thermal materials and in emerging field of phonon engineering.

Our prediction of the strong phonon interference effects at SAM interfaces can be compared against experimental results on interfacial conductance reported in Ref. 16. In Ref. 16 SAMs consisting of eight and ten carbon molecular chains were used and the interfacial resistance reported for the two cases were about the same within the experimental error. Nevertheless, some differences in interfacial conductance were observed, indicating that interfaces with longer chains have higher conductance. Such behavior is consistent with the phonon interference effects. In our modeling studies we vary the chain length by much larger factors that in the experiment. This might contribute to the fact that we observe more significant differences in interfacial thermal transport characteristics. Furthermore, our model system is idealized with all solid surfaces being atomistically smooth. This also enhances phonon interference effects. Furthermore, we need to point out that interfacial thermal resistance reported for metal—SAM interface is Ref. 16, which is of the order of 20 $\mathrm{MW/(m^2\,K)}$ is much lower than $100+\mathrm{MW/(m^2\,K)}$ estimated in Ref. 17. Both Refs. 17 and 16 assumed that strong thiol bonds exist at SAM-Au the interface. In reality, interfacial bonding quality might differ from the assumed one. In the case of the simulation, the interfacial bonding is fully characterized and can be varied in a controlled manner, allowing us to expose the role of SAM chains length on interfacial conductance.

ACKNOWLEDGMENTS

The work of L.H. and P.K. is supported by the U.S. Air Force Office of Scientific Research Grant No. MURI FA9550-08-1-0407. L.Z. and B.L. are supported by the Grant No. R-144-000-203-112 from Ministry of Education of Republic of Singapore. J.S.W. acknowledge support from a NUS research Grant No. R-144-000-257-112.

*Corresponding author; keblip@rpi.edu

[1] B. Li, L. Wang, and G. Casati, Phys. Rev. Lett. **93**, 184301 (2004); D. Segal and A. Nitzan, *ibid.* **94**, 034301 (2005); B. Hu, L. Yang, and Y. Zhang, *ibid.* **97**, 124302 (2006); N. Yang, N. Li, L. Wang, and B. Li, Phys. Rev. B **76**, 020301(R) (2007).

[2] C. W. Chang, D. Okawa, A. Majumdar, and A. Zettl, Science **314**, 1121 (2006).

[3] W. Kobayashi, Y. Teraoka, and I. Terasaki, Appl. Phys. Lett. **95**, 171905 (2009).

[4] B. Li, L. Wang, and G. Casati, Appl. Phys. Lett. **88**, 143501 (2006).

[5] L. Wang and B. Li, Phys. Rev. Lett. **99**, 177208 (2007).

[6] L. Wang and B. Li, Phys. Rev. Lett. **101**, 267203 (2008).

[7] L. Wang and B. Li, Phys. World **21**, 27 (2008).

[8] E. Hecht, *Optics* (Addison-Wesley, Reading, MA, 2001).

[9] J. M. Ziman, *Electrons and Phonons: The Theory of Transport Phenomena in Solids* (Oxford University Press, USA, 2001).

[10] V. Narayanamurti, H. L. Störmer, M. A. Chin, A. C. Gossard, and W. Wiegmann, Phys. Rev. Lett. **43**, 2012 (1979).

[11] M. Trigo, A. Bruchhausen, A. Fainstein, B. Jusserand, and V. Thierry-Mieg, Phys. Rev. Lett. **89**, 227402 (2002).

[12] Y. Ezzahri, S. Grauby, J. M. Rampnoux, H. Michel, G. Pernot, W. Claeys, S. Dilhaire, C. Rossignol, G. Zeng, and A. Shakouri, Phys. Rev. B **75**, 195309 (2007).

[13] N. D. Lanzillotti-Kimura, A. Fainstein, B. Jusserand, A. Lemaitre, O. Mauguin, and L. Largeau, Phys. Rev. B **76**, 174301 (2007).

[14] F. Schreiber, Prog. Surf. Sci. **65**, 151 (2000).

[15] E. T. Swartz and R. O. Pohl, Rev. Mod. Phys. **61**, 605 (1989).

[16] R. Y. Wang, R. A. Segalman, and A. Majumdar, Appl. Phys. Lett. **89**, 173113 (2006).

[17] Z. Ge, D. G. Cahill, and P. V. Braun, Phys. Rev. Lett. **96**, 186101 (2006).

[18] Z. H. Wang, J. A. Carter, A. Lagutchev, Y. K. Koh, N.-H. Seong, D. G. Cahill, and D. D. Dlott, Science **317**, 787 (2007).

[19] R. G. Nuzzo, L. H. Dubois, and D. L. Allara, J. Am. Chem. Soc. **112**, 558 (1990).

[20] H. Sun, S. J. Mumby, J. R. Maple, and A. T. Hagler, J. Am. Chem. Soc. **116**, 2978 (1994).

[21] F. Ercolessi, M. Parrinello, and E. Tosatti, Philos. Mag. A **58**, 213 (1988).

[22] R. Mahaffy, R. Bhatia, and B. J. Garrison, J. Phys. Chem. B **101**, 771 (1997).

[23] P. K. Schelling, S. R. Phillpot, and P. Keblinski, Appl. Phys. Lett. **80**, 2484 (2002).

[24] M. E. Lumpkin, W. M. Saslow, and W. M. Visscher, Phys. Rev. B **17**, 4295 (1978).

[25] L. Zhang, J.-S. Wang, and B. Li, Phys. Rev. B **78**, 144416 (2008).

[26] J. Velev and W. Butler, J. Phys.: Condens. Matter **16**, R637 (2004).

[27] M. Hu, P. Keblinski, and P. K. Schelling, Phys. Rev. B **79**, 104305 (2009).

[28] J.-S. Wang, J. Wang, and J. T. Lü, Eur. Phys. J. B **62**, 381 (2008).